Green Chemistry

PAPER

View Article Online
View Journal | View Issue

Cite this: *Green Chem.*, 2022, **24**, 4140

In silico COSMO-RS predictive screening of ionic liquids for the dissolution of plastic†

Mood Mohan, [a,b] Jay D. Keasling,[a,c,d,e,f,g,h] Blake A. Simmons [a,c] and Seema Singh *[a,b]

Plastic waste is currently produced at an alarmingly high rate, nearing 400 Mt per year. The accumulation of plastics in the environment is growing rapidly, yet our knowledge of their persistence is very limited. Efficient and affordable dissolution and chemical upcycling of plastic wastes are also a significant hurdle in the conversion of plastic polymers to value-added chemicals, and finding a suitable solvent is also a major concern. Ionic liquids (ILs) have recently demonstrated their ability to dissolve and convert polyethylene terephthalate (PET) into valuable products. However, identifying an optimal IL from the large number of anion and cation combinations possible is quite challenging. To address this issue, the COSMO-RS (COnductor-like Screening MOdel for Real Solvents) model has emerged as a reliable computational tool that can screen numerous ILs based on the different thermodynamic properties that are needed for polymer dissolution. The current study demonstrates the dissolution behavior of plastic wastes in ILs using the COSMO-RS model. In this study, 99 cations and 95 anions were chosen and combined to form 9405 ILs, which were evaluated by predicting logarithmic activity coefficient ($\ln(\gamma)$) and excess enthalpies (H^E) of typical plastic wastes (PET, polystyrene, polypropylene, and polyvinylchloride). Based on the COSMO-RS predicted thermodynamic properties ($\ln(\gamma)$ and H^E), anions such as acetate, formate, glycinate, and *N*-methylcarbamate in combination with the cations like superbase, ammonium, and pyrrolidinium are predicted to be suitable solvents for plastic dissolution. The predicted $\ln(\gamma)$ and H^E results are further validated with the experimental results and the predicted thermodynamic properties and experimental results are in good alignment. An excess enthalpy calculation demonstrated that strong hydrogen bond interactions between the polymer and the IL are vital factors for efficient dissolution to occur, with the anion and the cation of the IL having a similar effect on the process.

Received 22nd September 2021,
Accepted 13th December 2021

DOI: 10.1039/d1gc03464b

rsc.li/greenchem

1. Introduction

Plastics are ubiquitous in our everyday lives, and are relatively inexpensive materials that have been used to improve the quality of people's lives through food preservation and medical applications, among many others. However, the low production cost and an assortment of properties available have prompted an extreme reliance on these materials, especially for transient applications, resulting in a global plastic accumulation crisis.[1] The high demand for plastic has resulted in a tremendous growth in their production (over 400 MMT per year in 2018), with limited commercial methods in place to address the end-of-life challenges of these materials. Globally, 55% of plastic wastes end up in a landfill, while 20% are recycled, and 25% are burned for energy recovery.[2] A World Economic Forum report predicts that oceans will contain more plastics than fish by 2050.[3] The environmental consequences of this growth are frightful, as humans and animals are impacted in many ways.[4] The emergence of the coronavirus (COVID-19) pandemic has brought a dramatic increase in the

[a]*Deconstruction Division, Joint BioEnergy Institute, 5885 Hollis Street, Emeryville, California 94608, USA. E-mail: ssingh@lbl.gov, seesing@sandia.gov*
[b]*Department of Biomass Science and Conversion Technology, Sandia National Laboratories, 7011 East Avenue, Livermore, California 94551, USA*
[c]*Biological Systems and Engineering Division, Lawrence Berkeley National Laboratory, 1 Cyclotron Road, Berkeley, California 94720, USA*
[d]*QB3 Institute, University of California, Berkeley, California, 94720, USA*
[e]*Department of Bioengineering, University of California, Berkeley, California, 94720, USA*
[f]*Department of Chemical and Biomolecular Engineering, University of California, Berkeley, California, 94720, USA*
[g]*Novo Nordisk Foundation Center for Biosustainability, Technical University of Denmark, Building 220, Kemitorvet, DK-2800 Kgs, Lyngby, Denmark*
[h]*Center for Synthetic Biochemistry, Shenzhen Institutes for Advanced Technologies, Shenzhen, Guangdong, 518055, China*

†Electronic supplementary information (ESI) available: The chemical structures of anions (95) and cations (99), the COSMO-RS predicted logarithmic activity coefficient of PET in 9405 ILs, and the COSMO-RS predicted and experimental viscosity of ILs. See DOI: 10.1039/d1gc03464b

use of plastic materials such as masks, gloves, hand sanitizer bottles, medical suits, and test kits, which intensifies the problem.[5] Areas of importance include decreasing plastic consumption, preventing microplastic leakage, separating and processing post-consumer plastics, identifying sustainable replacements for disposable products, and enhancing recycling rates. "Breaking the Plastic Wave", a global analysis using first-of-its kind modelling, reports that reduction of plastic waste flow into the ocean by 80% possibly in the next 20 years with these combined efforts. Only 2% of plastic packaging in the United States is recycled in a closed-loop system, in which goods are recycled into similar-value products.[6]

The most promising chemical processes for converting polymers to their original monomers, fuels, or chemicals with potential for upcycled applications include chemical recycling and upcycling methods.[7] Developing more efficient methods for chemical recycling or chemical upcycling of plastics has become a critical area of research for numerous groups in chemistry and chemical engineering. A particular area of interest in this field is the discovery of novel solvents that can dissolve and depolymerize plastics at mild operating conditions, with high selectivity for value-added products. High dissolution of plastics is a critical step in conversion and recycling, but it is challenging. Success in this area could lead to a transformation of the commercial recycling market. A wide variety of approaches has been sought to dispose of several hundred million metric tons of synthetic polymers.[8,9] These include physical strategies,[8] biological degradation,[10,11] and chemical upcycling.[12] Among these approaches, chemical upcycling has gained widespread attention from both "sustainable society" and "green chemistry" to convert waste plastic into valuable chemicals.[13,14] Over the past few decades, ionic liquids (ILs), which are organic salts with a melting temperature lower than 100 °C, have emerged as potent solvents for (bio)polymer dissolution and depolymerization and have opened new opportunities for efficient (bio)polymer processing.[15] ILs exhibit several attractive properties such as negligible vapor pressure, non-flammable, non-toxic, high thermal and chemical stability, and its use as a catalyst for specific reactions. A slight modification in cation and/or anion structure results in an enormous range of potential ILs encompassing a wide variety of solvent properties. It has been demonstrated that the anion of IL plays a dominant role in the dissolution of (bio)polymers.[15,16]

Wang *et al.* (2009) reported the solubility of PET in 1-butyl-3-methylimidazolium chloride ([Bmim]Cl) at 180 °C with a solubility of 2.7 wt%.[17] Yue *et al.* (2011) conducted the glycolysis of PET using several basic ILs. Among different basic ILs, 1-butyl-3-methylimidazolium hydroxyl ([Bmim]OH) showed higher catalytic activity with 100% conversion of PET and 71.2% BHET yield at 190 °C and 2 h.[18] In another study by Yue *et al.* (2013) showed that the Lewis acidic IL ([Bmim]$ZnCl_3$) possesses high catalytic activity as compared to the neutral IL ([Bmim]Cl) in the glycolysis of PET. Significantly, the conversion of PET was achieved at 100% with low catalyst ([Bmim]$ZnCl_3$) loading (0.16 wt%).[19] Nunes *et al.* (2014) studied the depolymerization of PET in supercritical ethanol in the presence of 1-butyl-3-methylimidazolium tetrafluoroborate ([Bmim][BF_4]). The use of [Bmim][BF_4] and supercritical ethanol represented an auspicious combination for PET depolymerizations with a conversion of 98 wt% from PET to diethylterephthalate.[20] The methanolysis of polycarbonate (PC) over [Bmim][Cl] and [Bmim][OAc] was reported by Liu *et al.* (2010) and Song *et al.* (2013). The process could be performed under moderate conditions (105 or 90 °C). However, large amounts of ILs were needed to act together as a solvent at a high cost.[21,22] Wang *et al.* (2012 and 2015) reported that the H-bonds formed between PET-ILs and PET-EG were shown to play a critical role in the glycolysis of PET.[23,24] Further, Ju *et al.* (2018) investigated the microscopic degradation mechanism of PET in 24 different ILs by density functional theory (DFT). It has been observed that anion of IL plays a dominating role in the depolymerization of PET by forming new H-bonds with PET, while cations mainly attack the oxygen of carbonyl and have a π-stacking interaction.[25] Adams *et al.* (2000) have studied the catalytic cracking of polyethylene (PE) using 1-ethyl-3-methylimidazolium chloride–aluminum(III) chloride ([Emim]Cl–$AlCl_3$) to produce light alkanes (C3–C5 gaseous alkanes). Using ([Emim]Cl–$AlCl_3$) IL, HDPE produces 95% of gaseous alkanes and low-volatile cyclic alkanes at 120 °C and 72 h of reaction time.[26] In the computational and experimental literature, imidazolium-based cations are the most studied ILs for plastic (*e.g.*, PET) dissolution.[18,19,22,25,27] However, the imidazolium-based ILs are toxic to microbes,[28] and their application in the biodegradation of PET[29] will be challenging. There has been extensive literature on the glycolysis, aminolysis, alcoholysis, and hydrolysis of polyethylene terephthalate (PET) using ILs. However, a systematic ILs screening, theoretical understanding, and the development of a precise solvent for plastic has a significant potential. Fundamental understanding and development of a suitable and promising solvent for plastic dissolution by computational and experimental methods have immense potential.

Given the potential capabilities of these task-specific ILs, it is critical to understand the thermodynamic properties (*e.g.*, solubility, viscosity, and thermodynamic behavior) of neat ILs and their solutions with plastics. However, given the very large number of potential cations and anions to screen, it is impossible to study each possible IL anion–cation combination experimentally. Therefore, it is necessary to build sufficiently reliable theoretical approaches to screen the large number of ILs for plastic dissolution. Several predictive techniques have recently been developed and adapted for modeling the thermodynamic properties of systems containing ILs, such as the perturbed-chain statistical associating fluid theory (PC-SAFT),[30] group contribution methods,[31] quantitative structure–property relationship,[32] Monte Carlo molecular simulation,[33] molecular dynamics,[34] and COnductor-like Screening MOdel for Real Solvents (COSMO-RS).[35,36] Among these predictive techniques, the COSMO-RS model is a powerful tool for rapidly screening large numbers of ILs and has been widely used for the screening of ILs for different research

applications.[37–40] The ability to screen ILs using predictive methods that only require a minimal number of input parameters would result in significant time, cost, and effort reductions in laboratory studies.

For plastic dissolution, ionic liquids have shown some unique properties; but unlike ILs applications for lignocellulosic biomass, its utility for plastic dissolution is just beginning to gain attention in research. Much development works remains to be done, but as the technical challenges shift from fundamental scientific understanding to process-oriented engineering exploitation, the research priorities will be expected to evolve. Though the market for ionic liquids was well below the expectations in the last decade, there is an increasing number of encouraging trends. Most impressive is the 57 implemented ionic liquid applications known to date, which is a clear improvement compared to 13 in 2008.[41] There will be an optimistic future for ionic liquids, and "this is very much the end of the beginning regarding ionic liquid technologies, and not the beginning of the end". It was recently concluded that the ionic liquids field will soon reach maturity and enter the megatrend mass markets as a result of a survey (25 academic and industrial leaders) conducted by Roland Kalb at Proionic.[41]

Therefore, the present study aims to utilize the capabilities of the COSMO-RS model as an efficient tool in the screening and designing of potential ILs for plastic (*e.g.*, PET) dissolution. It is important to note that the COSMO-RS model has not, to the best of our knowledge, been employed to study plastic-IL systems. For the first time, the present study reports the use of COSMO-RS model to screen the robust ILs for plastic dissolution. In this study, 99 cations (both aromatic and non-aromatics) and 98 anions (hydrophilic and hydrophobic) were screened for polyethylene terephthalate (PET) dissolution, thereby selecting better ion combinations based on the activity coefficient and excess enthalpy values. Further, this study also investigates the screening of ILs for other plastics such as polypropylene (PP), polystyrene (PS), and polyvinylchloride (PVC). Moreover, the viscosity of selected ILs has also been predicted to identify an optimal IL.

2. Computational details

2.1. COSMO-RS calculations

The COSMO-RS calculations were carried out following multiple simulation steps. First, the geometries of all the investigated plastic molecules such as polypropylene (PP), polyethylene (PE), polyvinylchloride (PVC), polyethylene terephthalate (PET), polyurethanes (PUE), and polystyrene (PS), and ions (anions and cations) of ionic liquids were drawn in the Avogadro freeware software.[42] Gaussian09 package was used to optimize the geometries of investigated molecules at B3LYP (Becke 3-parameter hybrid functional combined with the Lee–Yang–Parr correlation) theory and 6-311+G(d, p) basis set. The frequency calculations were also performed to verify the reasonability of the optimized structures and energy minima.[43–45] After successful geometry optimization, the next step is to generate the COSMO file using the BVP86/TZVP/DGA1 level of theory and basis set.[39,46,47] The combination of TZVP and DGA1 basis sets allows the electron density to adjust spatially to the extent appropriate to the particular molecular environment. The ideal screening charges on the molecular surface were then computed using the same level of theory BVP86 *via* the keyword "scrf = COSMORS".[48,49] The generated COSMO files were then used as the input in the COSMOtherm (version 19.0.1, COSMOlogic, Leverkusen, Germany) package.[50,51] BP_TZVP_19 parametrization was used to calculate the sigma profiles, sigma potentials, viscosity, partition coefficient of the isolated molecules, and excess enthalpy (H^E) and logarithmic activity coefficients ($\ln(\gamma)$) of binary mixtures.

The calculation of excess enthalpy of a mixture can be predicted by using the following eqn (1):[47]

$$H_m^E = \sum x_i H_i^E = \sum x_i [H_{(i,\text{mixture})} - H_{(i,\text{pure})}] \quad (1)$$

where, $H_m{}^E$ is the excess enthalpy of each molecule in the mixture, defined as the enthalpy difference between component i in the mixture and in the pure state.

On the other hand, excess enthalpy of a mixture is an algebraic sum of three contributors (eqn (2)) associated with the electrostatic misfit, hydrogen bonding, and van der Waals forces.

$$H_M{}^E = H_M{}^E(\text{misfit}) + H_M{}^E(\text{H-bond}) + H_M{}^E(\text{vdW}). \quad (2)$$

And the activity coefficient of component i is related to the chemical potential μ_i is given as:[52,53]

$$\ln(\gamma_i) = \left(\frac{\mu_i - \mu_i{}^0}{RT}\right) \quad (3)$$

where $\mu_i{}^0$ is the chemical potential of the pure component i, R is the real gas contact, and T is the absolute temperature. More details of COSMO-RS calculation in predicting the excess enthalpies and activity coefficients are provided in the COSMOtherm's user Manual.[54]

It should be mentioned that the polymeric structures can exhibit multiple conformations. Obtaining the most stable conformer of polymers is computationally more expensive and time-consuming. However, there are several ways to represent a polymer with the COSMOtherm. Only for a low degree of polymerization it is computationally feasible to use the complete molecule. To model a polymer in the COSMO-RS calculations, the end group of the polymer (*e.g.*, PET) is deactivated using a function called "weight string", which allows for selectively switching on/off certain atoms within a COSMOfile. The weight string function has been widely applied to the polymer (repeated unit) molecules in the literature. Loschen and Klamt used a mid-trimer of polyethylene glycol as a polyethylene glycol polymer structure.[55] Further, Kahlen *et al.*, Liu *et al.*, Casas *et al.*, and Huang *et al.* modeled mid-monomer of cellotriose and mid-dimer of cellotetraose to represent the cellulose model polymeric structure in COSMO-RS calculations to screen the hundreds of ionic liquids.[39,56–58] Thus, a similar

weight string function was used for plastic molecular simulations in the COSMO-RS calculations (see Fig. S1†).

2.2. Structures of ionic species

The chemical structures of anions and cations of ionic liquids employed in this work can be seen in Tables S1 and S2,† respectively. The COSMO files of all the cations and anions were generated based on the procedure outlined in section 2.1. According to Wang *et al.* (2012) and Mohan *et al.* (2018), imidazolium-based and pyridinium-based ILs with functional groups alkyl-, allyl-, hydroxyl-, ether-, and ester- have the potential capability to dissolve polymers.[40,59] Morpholinium-based and pyrrolidinium-based ILs with these functional groups were accounted based on the works of Raut *et al.* (2015), Kahlen *et al.* (2010), and Zavrel *et al.* (2009).[56,60,61] Based on the Kahlen *et al.* (2010) and Balaji *et al.* (2012), guanidinium and ammonium-based cations with different functional groups are considered.[56,62] Further, the superbase-based cations are accounted for based on the study of Kuzmina *et al.* (2017), which reports that superbase-based ILs are potential candidates for the dissolution of polymeric compounds.[63] On the other hand, Liu *et al.* (2018) studied the alcoholysis of polycarbonate (PC) with superbase ionic liquids and reported that 99% of bisphenol A (BPA) yield and 100% of PC conversion.[64] The anions such as amino acid-based anions are considered for the screening study based on the Ohno and Fukumoto (2007) study.[65] In this work, a total of 99 cations and 95 anions resulting in the 9405 ILs are studied for plastic dissolution.

3. Results and discussion

3.1. Benchmarking study

The COSMO-RS model is a powerful thermodynamic tool for the screening of solvents for polymer dissolution. Only structural information is typically required for COSMO-RS to predict the solubility and other thermodynamic properties. In our earlier work on lignocellulosic biomass, we have successfully shown the applicability of COSMO-RS predicted activity coefficients (γ) against experimental solubility of biomass components in ILs and screened thousands of ILs for biomass dissolution.[16,40,46] However, a separate benchmark study was also performed for plastic (*i.e.*, PET) conversion in ILs, and the results are depicted in Fig. 1 and 2. It is worthwhile to mention that the COSMO-RS predicted thermodynamic properties such as activity coefficient and excess enthalpies are critical parameters in determining the ability of a solvent on the solute's dissolution. The activity coefficient and excess enthalpies are related to the solubility and interaction between unlike species, respectively. The lower activity coefficient (γ) and excess enthalpies (H^E) of a solute in the solvents indicate that solvent has a greater tendency to interact and solubilize the solute. Fig. 1 illustrates the COSMO-RS predicted ln(γ) against known experimental PET conversion data which was taken from the literature.[27] It was observed that the ILs had

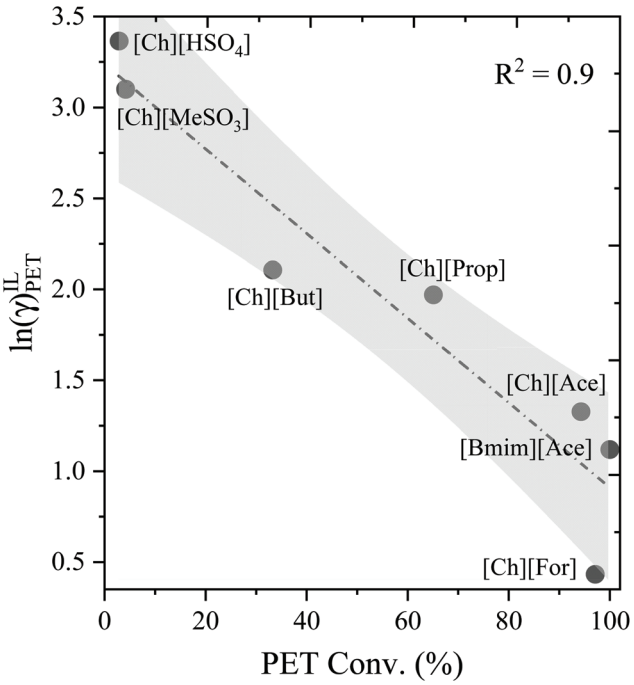

Fig. 1 Correlation between COSMO-RS predicted activity coefficient and experimental PET conversion.

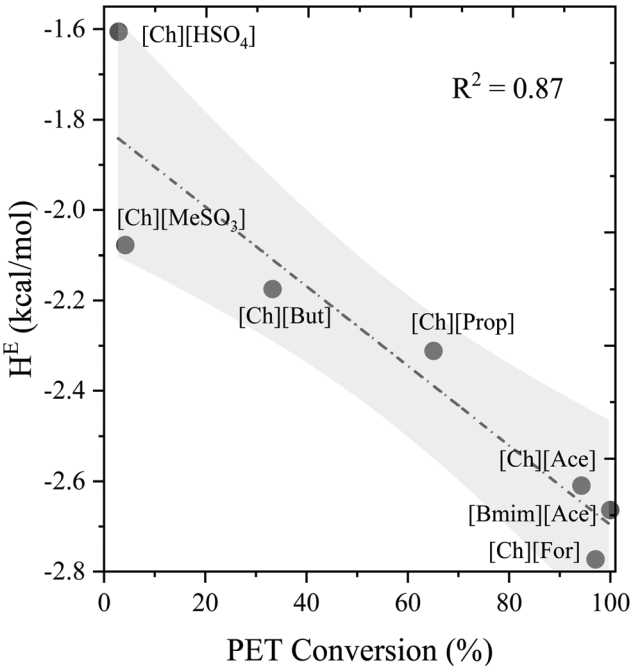

Fig. 2 Correlation between COSMO-RS predicted excess enthalpy and experimental PET conversion.

shown lower ln(γ) value results in a higher conversion of PET. On the other hand, Fig. 2 demonstrates the correlation between COSMO-RS predicted excess enthalpy against experimental PET conversion. Similar to ln(γ), a lower value of H^E

results in a higher conversion of PET in ILs. Results of the above validation show a good correlation between COSMO-RS predicted thermodynamic properties and experimental PET conversions in ILs. Therefore, after an extensive benchmarking study, we can now screen thousands of IL solvents for plastic dissolutions/conversion.

3.2. Sigma profile and sigma potentials of plastics

To understand the polarity and reactivity of plastic molecules, sigma (σ)-potentials of the isolated plastic molecules were calculated using the COSMO-RS model. The σ-potential is a measure of the affinity of the system to a surface of polarity σ, which provides insights into a plastic interaction with itself and with solvent. The chemical configuration and screening charge distribution on the PET molecule are shown in Fig. S1.† This screening charge distribution data was used to determine the thermodynamic properties of investigated plastic polymers and ILs, and the distribution plots of σ-potentials and σ-profiles are presented in Fig. 3 and S2,† which were then used to compute the intra- and intermolecular interactions. The σ-profiles and σ-potential is divided into three regions: H-bond acceptor (red: $\sigma > +0.01$ e Å^{-2}), H-bond donor (blue: $\sigma < -0.01$ e Å^{-2}), and non-polar (green: -0.01 e Å$^{-2} < \sigma > +0.01$ e Å^{-2}) regions. Fig. 3 depicts the σ-potentials of different plastic substrates. On the negative side of screening charge density (SCD: $\sigma > -0.01$ e Å^{-2}), the σ-potential ($\mu(\sigma)$) value of PET and polyurethane is more negative, which implies that PET and polyurethane have more affinity to interact with the H-bond donor surfaces. In contrast, the $\mu(\sigma)$ value is positive in the region of large positive screening charge density ($\sigma > +0.01$ e Å^{-2}), which reflects PET lack of H-bond donor surfaces, this indicates the intramolecular interaction in PET is weak, which enables to interaction with hydrogen donor surfaces of solvent. On the other hand, the $\mu(\sigma)$ of polyurethane is negative, indicating that PUE could interact with both H-bond donor and acceptor molecules. Whereas in the case of PP, PE, PS, and PVC, the σ-potential ($\mu(\sigma)$) values are positive in both negative and positive screening charge densities, implying that these plastic polymers do not participate in polar interactions, their most favorable interactions through hydrophobic, π–π, cation–π, and CH–π interactions.

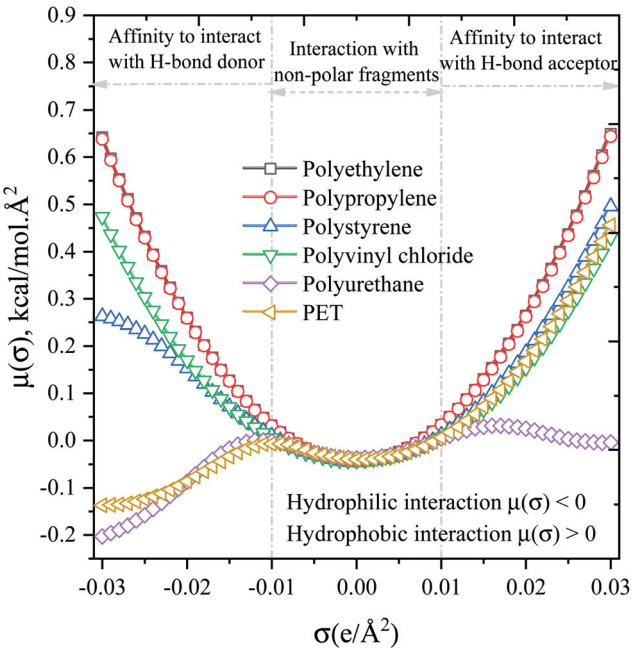

Fig. 3 Sigma potentials of different plastics predicted by COSMO-RS.

3.3. Screening of ionic liquids

As per the standard definition, ILs can be freely combined from organic cations and organic/inorganic anions, thereby forming numerous candidates for plastic dissolution (or polymers). It should be noted that experimental studies become expensive and time-consuming without a screening of potential solvents. The COSMO-RS model is a thermodynamics tool that was used to predict the useful thermodynamic properties such as logarithmic activity coefficient $\ln(\gamma)$ and excess enthalpy H^E of binary mixtures (*i.e.*, plastic-ILs). In the present study, 99 cations and 95 anions comprising 9405 combinations were screened for PET and ranked based on their $\ln(\gamma)$ and H^E values (Fig. 4 and 5). Initially, the ILs were screened for PET because extensive literature was available on PET solubility (or conversion) in ILs. Thus, our preliminary study focused on PET to test and validate experimental PET data using the COSMO-RS model (Fig. 1 and 2). The structures and properties of 99 cations and 95 anions were presented in the ESI (Tables S1 and S2†). At this point, it should be important to mention that most of the ionic liquids are liquid at room temperature (RT), but some of them are solid at RT, generally have a melting point lower than 100 °C. In order to study the effect of RTILs and non-RT ILs (<100 °C), the COSMO-RS calculations have been performed at 90 °C for screening study. In the literature, it has been reported that dissolution and conversion of plastic polymers requires elevated reaction conditions (higher temperature and time).[18–21,26] However, ILs have the potential to lower the processing temperature and even enable room temperature dissolution.

Activity coefficient and excess enthalpy values are often used as a quantitative descriptor for the dissolution power of a solvent. According to the solid–liquid equilibria (SLE) assumptions,[48,66] the reciprocal of the activity coefficient and excess enthalpy characterize a PET's solubility in the respective IL. Cations and anions were sorted according to their dissolving capacity and arranged in such a way that ILs with high dissolving power (*i.e.*, $\ln\gamma$ and $H^E \ll 0$) of PET are situated in the left and bottom portion of Fig. 4 and 5, and the weaker ones (*i.e.*, $\ln\gamma$ and $H^E > 0$) are situated at the top portion and right side of Fig. 4 and 5. The anions such as acetate, formate, glycinate, glycolate, and *N*-methylcarbamate are predicted to dissolve the PET more efficiently in combination with the cations like superbase, tetraalkylammonium, and tetraalkylphosphonium. This is due to the fact that ILs form strong H-bonds, π–π, and cation–π interactions with PET. However, the anions such as $[PF_6]^-$, $[BF_4]^-$, triflate, gentisate, histidi-

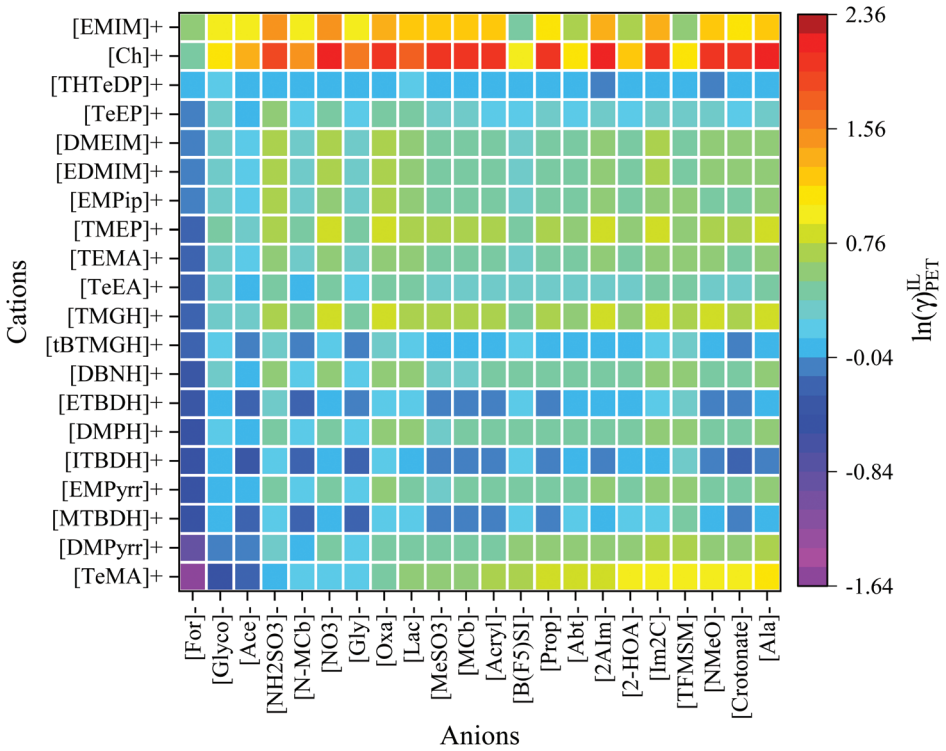

Fig. 4 Graphical representation of the logarithmic activity coefficients of PET in different ILs at 363.15 K by COSMO-RS model.

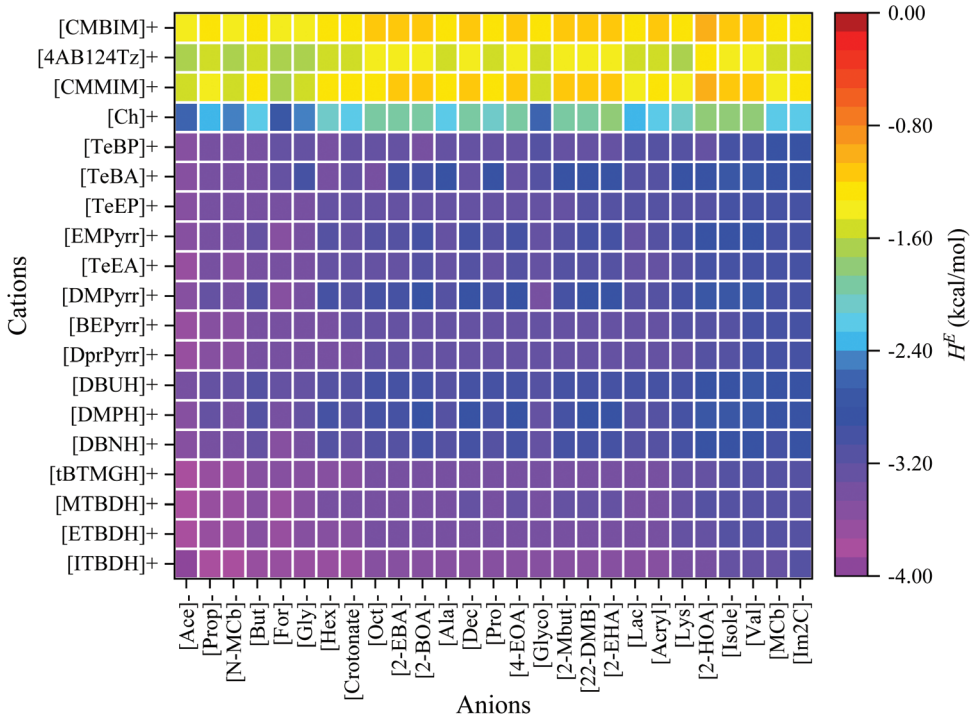

Fig. 5 Graphical representation of the excess enthalpy of PET in different ILs at 363.15 K by COSMO-RS model.

nate, and bis(trifluoromethylsulfonyl)imide have very high values of ln γ. The activity coefficient values of PET in 9405 ILs are provided in Table S3.†

As the size of the cation increases, both logarithmic activity coefficient and excess enthalpy of PET was seen to decrease (Table S3†). For example: the alkyl chain length of the

ammonium ($[MTOA]^+$, $[TeBA]^+$, $[TeEA]^+$, and $[TeMA]^+$) and imidazolium-based ($[DMIM]^+$, $[EMIM]^+$, $[PMIM]^+$, $[BMIM]^+$, $[HMIM]^+$, and $[OMIM]^+$) cations increases, the $\ln\gamma$ and H^E were seen to be decreasing with amino acid-based anions. On other hand, the $\ln\gamma$ of PET was observed to be lower as the alkyl chain length of the anions increased. For example: the alkyl chain length of carboxylate anion increases ($[Prop]^-$, $[But]^-$, $[Hex]^-$, $[Oct]^-$, and $[Dec]^-$), the $\ln\gamma$ of PET is decreased. A similar observation was also seen in superbase-based cations. As the alkyl chain length of superbase cations increases ($[MTBDH]^+$, $[ETBDH]^+$, and $[ITBDH]^+$), the $\ln\gamma$ of plastic polymer was seen to be lower. However, the combination of smaller size cation and anion results lower $\ln\gamma$ and H^E of PET than smaller size cation and larger size anion or *vice versa*. For instance, the combination of tetramethylammonium $[TeMA]^+$ and tetraethylammonium $[TeEA]^+$ cations with formate $[For]^-$ and acetate $[Ace]^-$ anions, results lower $\ln\gamma$ of PET (Table S3†) than larger cation sizes ($[TeBA]^+$ and $[MTOA]^+$). The combination of lower size ions possesses enhanced IL polarity and stronger hydrogen bonding acceptor and donor capability to solvate a plastic polymer.

The ions of IL should obey the following successive criteria: (1) either of the ions should be a good hydrogen bond acceptor or donor, and (2) another ion to be slightly polar (to weakly coordinate with counter ion thereby reduces the cross interactions between anion and cation). According to this thumb rule, the cations such as superbase, tetraalkylammonium, and tetraalkylphosphonium are less polar, and the anions such as acetate, formate, glycinate, glycolate, and *N*-methylcarbamate are highly polar in nature. Thus, the interaction between the polar anion and the PET is energetically much stronger than the interaction between anion and cation, resulting in a high PET solvation capability.

3.4. Excess enthalpy of PET in ILs by COSMO-RS

As discussed earlier, the excess enthalpy corresponds to the intermolecular interactions (misfit, H-bonds, and van der Waals energies) between the plastic polymer and selected seven ILs were calculated by the COSMO-RS model and depicted in Fig. 6. It is worth noting that if the excess enthalpy of plastic in ILs is negative, the process is exothermic, and plastic dissolution in ILs is favorable. The histogram in Fig. 6 demonstrates that the H-bond interaction energy between PET and the cations and anions of IL have shown a greater influence on the dissolution capability of PET in the ILs, and then followed by misfit and vdW interactions. For ILs with same anion and different cations, such as [ITBDH][Ace], [DBNH][Ace], and [Emim][Ace], the values of excess enthalpies are different. On the other hand, the ILs with same cation (*e.g.*: $[ITBDH]^+$) and different anions exhibit different excess enthalpy values as well. This ascription indicates that both anion and cation of the ILs play a vital role in the dissolution and conversion of PET. These results agree with the study of Ju *et al.* (2020), which reported that anion plays an important role in the dissolution of PET.[25] However, when the hydrogen atom of the methyl group is replaced by hydroxy or carbonyl group,

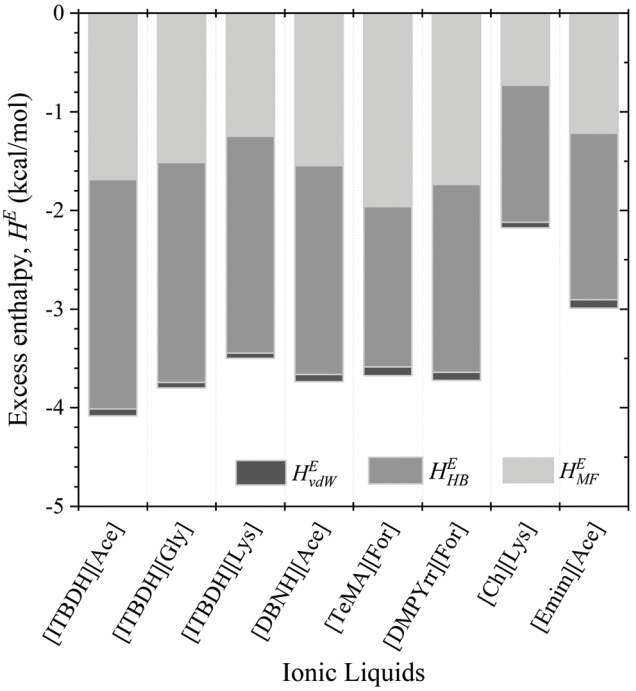

Fig. 6 Energetic contributions to the excess enthalpy of the binary mixtures between PET and eight selected ILs predicted by COSMO-RS at T = 363.15 K.

the interaction between amino acid-based anion and PET becomes weaker. A similar observation was also noticed in our study as well. For example, in a comparison made between the acetate and glycinate anions with $[ITBDH]^+$, the excess enthalpy of PET was seen to be decreased. For cations, the interaction (H^E) between PET and ILs decreased as an increase in the alkyl chain length of the cation. It was also reported that anion of the IL forms multiple H-bonds with PET. At the same time, cations mainly attack the oxygen atom of carbonyl (*i.e.*, H-bond) and have a π-staking interaction with PET, thereby increases the dissolution of PET. The results of Ju *et al.* (2018)[25] are in line with the COSMO-RS predicted excess enthalpies where H-bonding energy plays a leading role.

Yao *et al.* (2021) performed the DFT calculations to understand the effect of amino acid-based ionic liquids on the degradation of PET.[67] It has been reported that amino acid-based ILs ([Bmim][Pro]) forms multiple hydrogen bonds with PET, which leads to the higher conversion of PET and suggests that amino acid-based ILs have the potential capability to degrade PET. In our study, amino acid-based ILs are also predicted to be better solvents for PET, and the results agree with Yao *et al.* (2021).[67] The present study predicted excess enthalpy values of PET in ethylene glycol + ILs were also compared with the experimental conversion of PET and found that the COSMO-RS predicted H^E and experimental PET conversion are in good agreement (Fig. 2), and thus confirms that our COSMO-RS predicted results agree with experimental data.

3.5. σ-Profiles of anions and cations by COSMO-RS

The activity coefficient and excess enthalpy results demonstrated that both anion and cation significantly influence the PET dissolution process. The sigma profiles of anions and cations were calculated to understand the possible interactions between the PET and ions of ILs (Fig. 7). As discussed earlier, the sigma profile of PET distributed in the non-polar (green: -0.01 e Å^{-2} < σ > $+0.01$ e Å^{-2}) and H-bond acceptor regions (red: $\sigma > +0.01$ e Å^{-2}). From Fig. 7a, the peaks of [ITBDH]+ and [DBNH]+ were located in the H-bond donor regions (blue: $\sigma < -0.01$ e Å^{-2}) indicates the ability of cations to act as H-bond donors. While the σ-profile of anions lie in the positive screening charge density ($\sigma > +0.01$ e Å^{-2}) indicates that H-bond acceptor. From the σ-profile point of view, the superbase cations form stronger hydrogen bonds and cation–π interactions with PET, while the anions could form multiple hydrogen bonds with the PET. Based on the results of Ju *et al.* (2018),[25] the strength of the H-bond acceptor and donor interactions are stronger between PET dimer and anions of IL. It is also important to mention that the σ-profile of cholinium lies in both the H-bond donor and acceptor regions, indicating that cholinium can interact with PET. However, the IL cholinium lysinate ([Ch][Lys]) was predicted to be a mild solvent for the dissolution of PET. This is because both cholinium and lysinate ions are polar in nature and the interactions between anion and cation were stronger thereby increasing the viscosity of [Ch][Lys] IL. On the other hand, when we take a closer look at Fig. 7b, the polarity of $[Gly]^-$ and $[Lys]^-$ are higher than $[Ace]^-$ anion ($\sigma = 0.014$ e Å^{-2}), which results in stronger interactions between cation $[ITBDH]^+$ and anions. Therefore, the excess enthalpy of PET in [ITBDH][Ace] is stronger than [ITBDH][Gly] and [ITBDH][Lys].

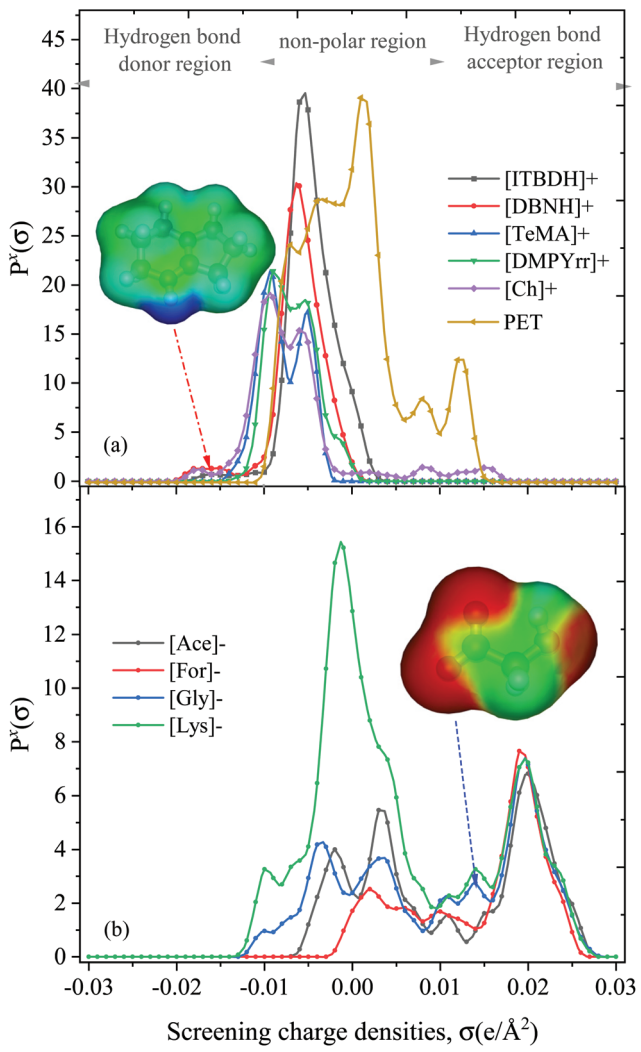

Fig. 7 Sigma profiles of (a) cations/PET and (b) anions of IL. In the COSMO cavity (charge distribution), red, blue, and green colors represent the negative, positive, and neutral charge on the molecule's surface, respectively.

3.6. Activity coefficient of PS, PVC, and PP in ILs

After successful screening of thousands of ILs for PET, now we further predicted the logarithmic activity coefficient for other plastic polymers in the top (*i.e.*, better) ranked ILs which was selected based on the Fig. 4 and 5. Plastic polymers such as polystyrene (PS), polyvinylchloride (PVC), and polypropylene (PP) are considered, and the results are illustrated in Fig. 8(a–c). Here, it is important to mention that the ILs were not screened for polyethylene (PE) due to the PP and PE exhibit similar structures (Fig. 3); thus, the IL screening study was not conducted for PE. Cations and anions were sorted according to their dissolving capacity and arranged in such a way that ILs with high dissolving power (*i.e.*, $\ln\gamma < 0$) of plastic polymers are situated in the left and bottom portion of Fig. 8, and the weaker ones (*i.e.*, $\ln\gamma \gg 0$) are at the top portion and right side of Fig. 8. The anions such as acetate, formate, glycinate, and *N*-methylcarbamate are predicted to be good solvents for plastic polymers in combination with the cations like $[TeMA]^+$, $[DMPyrr]^+$, $[MTBDH]^+$, and $[ITBDH]^+$. Similar ion combinations were also found to be better ILs for PET dissolution. Therefore, the present study offers not only the development of ILs for individual polymers it also demonstrates the predicted ILs could dissolve bulk plastic material.

3.7. Viscosity of ionic liquids

Apart from the interaction energies, the viscosity of solvent also plays an essential role in the dissolution of a polymer. The higher viscosity of a solvent can limits the effective mass transfer rate, which is known to have a negative effect on the polymer dissolution.[40,68,69] The solvents with lower excess enthalpy, H^E and activity coefficient values of polymer should also be cross-checked for viscosity of a solvent. Therefore, the viscosity of superbase, ammonium, and pyrrolidinium-based ionic liquids was predicted using the COSMO-RS model. For calculating the viscosity using COSMO-RS model, the conformers of each ionic liquid were generated using the Turbomole[70,71] and COSMOconfX packages, and the predicted viscosities are summarized in Table S4† (benchmark) and Fig. 9. From Fig. 9, the viscosity of amino acid-based ionic

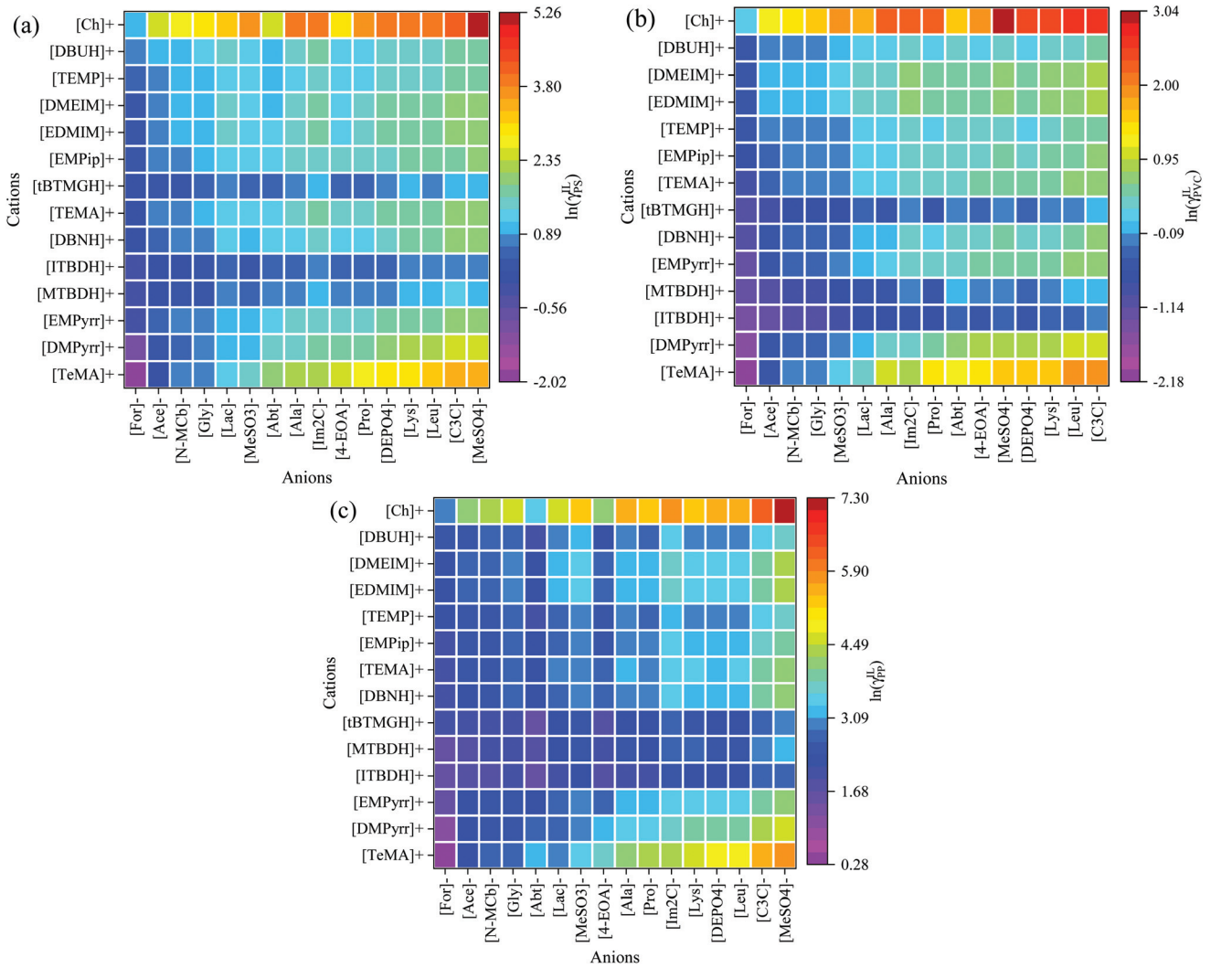

Fig. 8 Graphical representation of the logarithmic activity coefficients of plastic polymers (a) PS, (b) PVC, and (c) PP in different ILs at 363.15 K by COSMO-RS model.

liquids had a higher viscosity than carboxylated-based ($[Ace]^-$, $[For]^-$, and $[N\text{-}MCb]^-$) ionic liquids. It has been reported that as the alkyl chain lengths of the cation or anion increase, the viscosity of ionic liquids was reported to be increased and the H-bond acidity was decreased.[72] The similar pattern was also observed in our study. As the alkyl chain length of the anion increases, the viscosity of amino acid-based ILs (*e.g.*: [DBNH][Lys], [DBNH][Leu], and [DBNH][Gly]) were seen to be increased. ILs with the same anion (*e.g.*, $[Gly]^-$ and $[Ace]^-$) and different cations, the viscosity of ammonium and pyrrolidinium-based cations has shown higher viscosity than superbase-based ILs. On the other hand, the viscosity of superbase-based ILs were predicted to be lower than the traditional ionic liquids such as imidazolium, ammonium, and pyrrolidinium-based ILs. It was also reported that ILs with an adequate polarity and a low viscosity demonstrate an excellent ability to dissolve the polymer in a short residence time.[69,73] Jehanno *et al.* (2018) studied the glycolysis of PET using superbase IL (1,5,7-triazabicyclo[4.4.0]dec-5-enium methanesulfonate) and archived the BHET yield of 91%.[74] The synthesis of superbase ILs is more straightforward than the aprotic and traditional ILs synthesis procedure. Therefore, certain room-temperature superbase ILs that depicted low viscosity were superior to some imidazolium-based ILs. The development of room-temperature superbase ILs with low viscosity is of significant practical importance for the technological process in plastic upcycling.

On the other hand, the addition of a co-solvent to the IL may have a significant impact on the plastic dissolution by lowering the viscosity of IL and promotes the rate of mass transfer. From our previous study on the effect of protic and aprotic co-solvents on the dissolution of cellulose in ionic liquids,[68] we observed that addition of aprotic solvent to IL enhances the cellulose solubility while the protic solvents decrease the cellulose solubility.[68,69,74] It has been revealed that aprotic solvents interact with cation of IL, the free counter

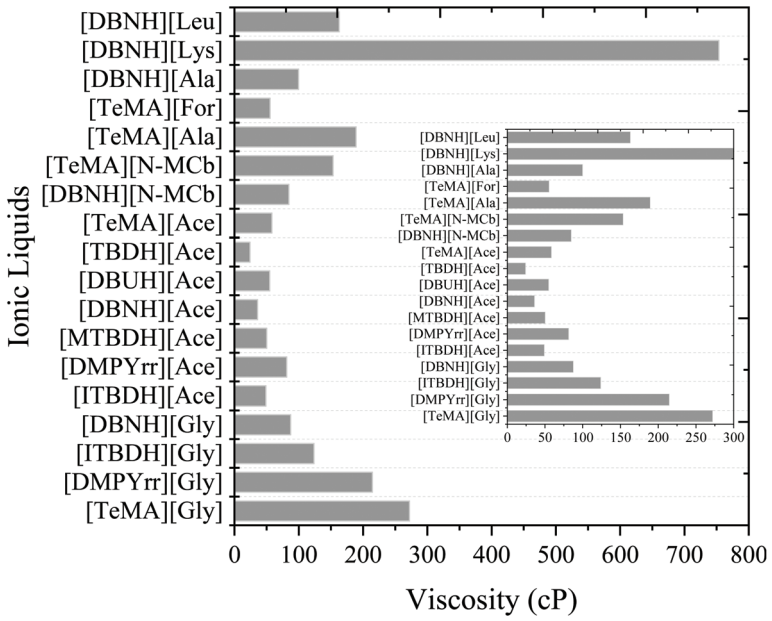

Fig. 9 COSMO-RS-based predicted viscosities of investigated ionic liquids.

anions in the system strongly interact with cellulose thereby enhances the cellulose solubility. Whereas in the case of protic solvent system, protic solvents strongly interact with anion of the IL which hinders the cellulose-anion interactions and decreases cellulose solubility. Similarly, co-solvent mechanism could be applicable for plastic dissolution as well.

3.8. Toxicity of ionic liquids

In the European Union, a substance sold in excess of one ton per year (tpa), Registration, Evaluation, Authorization and Restriction of Chemicals (REACH) is required, and overseas markets will require similar registration.[75–77] Because of extremely low volatility, ionic liquids were generally referred to as "green solvents". Most ionic liquids are environmentally friendly, but some of them are toxic, non-biodegradable, or even enduring and bio-accumulative. As a result, as soon as an ionic liquid becomes a commercial product, it must undergo the region-specific test protocols (*e.g.*, REACH aimed at protecting human health and the environment). However, there is still a need for more information on ILs' health and environmental safety data. The sheer number of ionic liquids conceivable, as well as their extremely diverse chemical structures, it is impossible to make broad statements about their health and safety implications. Each specific class of ionic liquids needs to be evaluated in depth based on their own intrinsic and extrinsic ecotoxicity and cytotoxicity profiles.

The interaction of ILs with cellular membranes determines their toxicity, which is primarily determined by the type of IL (alkyl chain length, cation family, and anion moiety) and the morphology of the model organisms. Recently, Kebaili *et al.* (2020) performed the toxicity analysis of 69 ionic liquids on *Shewanella* sp. microorganism. The ILs analyzed in their study were based on the cation's imidazolium, pyridinium, pyrrolidinium, piperidinium, morpholinium, oxazolinium, phosphonium, ammonium, and sulfonium, in combination with different anions. It was discovered that a reduction in the alkyl chain's hydrophobicity was a critical factor in lowering IL's toxicity. On the other hand, it was also reported that the *Shewanella* Sp. microorganism was largely incompatible with ILs with long alkyl chains that contained phosphonium-based cations.[78] Although it was previously assumed that the cation was the primary cause of toxicity, however, the importance of the anion should not be overlooked. Cho *et al.* (2008) reported the toxicity of [Bmim]-based cation with different anions such as Br^-, Cl^-, $[BF_4]^-$, $[PF_6]^-$, $[CF_3SO_3]^-$, $[C_8H_{17}SO_4]^-$ and $[SbF_6]^-$ on *Selenastrum capricornutum*. Expect for $[PF_6]^-$ (EC_{50} 1318 μM) and $[SbF_6]^-$ (EC_{50} 135 μM) all other ILs have shown low toxicity (EC_{50} 2137–2884 μM) on *Selenastrum capricornutum*.[79] Santos *et al.* (2015) studied the toxicity of ten cholinium-based ionic liquids by varying the functionalization of anion and cation structures. It was reported that structural changes in the ILs results differences in toxicity highlighting the importance of the role of the anion in their toxicity. The addition of phenolic group to [Ch][Ace] IL results higher toxicity of [Ch][Sal].[80] IL toxicity was usually induced by fluorinated anions like $[BF_4]^-$, $[PF_6]^-$, and $[SbF_6]^-$, which could be due to their ability to undergo hydrolysis in water.[81]

A cation, which is known to be nontoxic in one compound, combined with an anion, which is known to be nontoxic in another compound, does not guarantee the formation of a nontoxic substance. It is therefore necessary to test each new cation–anion combination individually. Approaches to structural modification that can result in nontoxic and biodegradable ILs and can be used to create more "environmentally friendly solvents". Coleman and Gathergood (2010) proposed that introduction of polar functional groups to alkyl

side chains significantly decreases the toxicity. The addition of a methyl or hydroxymethyl group to an imidazolium ring boosts its antimicrobial properties. The inhibitory effect of aprotic IL (EC_{50} 8.59–14.4 μM) were shown to be more significant than protic ILs (EC_{50} 302–8912 μM) towards acetylcholinesterase.[77] Thus, protic ILs, ions with short alkyl chains, or cholinium cations are recommended as environmentally friendly ILs.

3.9. Ionic liquids recycling

Ionic liquids have been studied and used in a variety of fields, including catalyst processing, biomass deconstruction, polymer dissolution, material synthesis, extraction, desulfurization, and hydrogenation, among others.[82] However, because of their hygroscopicity or ability to dissolve in solvents, they are frequently contaminated by various solutes and solvents. Ionic liquid recovery and purification are currently one of the biggest challenges to address before they can be used in industrial applications.[83] There have been a number of different technologies investigated over the last few decades for the recovery and purification of ILs at the lab and pilot scale for the recovery and purification of ILs.[84] These technologies include distillation, extraction, adsorption, membrane separation, aqueous two-phase extraction, crystallization, and external force field separation.[83] Even though some methods are capable of separating ionic liquids from solutions, their efficiencies are often limited, resulting in reduced product purity or high costs or high energy input. Effort should be made to improve the ionic liquid recovery process in the future. There is a need for more in-depth and comprehensive fundamental research into separation technologies, such as thermodynamic and kinetic analysis in distillation and adsorption, optimization of mass and heat transfer during extraction, exploration of the deactivation and regeneration mechanisms of the membrane, energy optimization of the separation processes, and so on. In contrast, a combined recovery process is an attractive route for the recovery of ILs.

4. Conclusions

A detailed fundamental understanding of plastic dissolution is still lacking, *in silico* screening of solvents could establish the structure–activity relationship and general guidelines for designing solvents and its application in plastic upcycling. Therefore, the present study reports the screening of robust ionic liquids for the dissolution of plastic wastes using the COSMO-RS model. A total of 9702 ILs (combination of 99 cations and 98 anions) were screened for plastic by predicting the fluid mixture properties. The prediction of thermodynamic properties such as logarithmic activity coefficient ($\ln(\gamma)$), excess enthalpies (H^E), and viscosity of ILs are critical factors that determine the dissolution efficiency of a given IL. Based on the prediction results of the plastics, it can be concluded that anions such as acetate, formate, glycinate, and *N*-methylcarbamate in combination with the cations like $[TeMA]^+$, $[DMPyrr]^+$, $[MTBDH]^+$, and $[ITBDH]^+$ are predicted to suitable solvents for plastic dissolution. It has been found that the H-bond interaction energy between plastic and the IL has shown more significant influence on the dissolution plastic in the ILs, and then followed by misfit and vdW interactions, and the anion and cation of IL were seen to have a similar effect on plastic dissolution process. The COSMO-RS predicted results were validated with the experimental results and found a good agreement between them. It was found that ammonium and pyrrolidinium-based ionic liquids were marginally better solvents than superbase-based ILs. Further, the viscosity of ILs was also predicted, and it was predicted that the superbase-based ILs would be less viscous than the traditional ILs and easier to handle. The synthesis of superbase ILs is simpler than that for aprotic and traditional ILs. Therefore, the design of room-temperature superbase ILs with low viscosity has significant potential in the development of an efficient plastic upcycling process. The present study offers the development of ILs not only for individual plastic polymers but also demonstrates the predicted ILs could dissolve bulk plastics.

Conflicts of interest

The authors declare no competing financial interest.

Acknowledgements

This work was part of the DOE Joint BioEnergy Institute (http://www.jbei.org) supported by the U. S. Department of Energy, Office of Science, Office of Biological and Environmental Research, through contract DE-AC02-05CH11231 between Lawrence Berkeley National Laboratory and the U. S. Department of Energy. The United States Government retains and the publisher, by accepting the article for publication, acknowledges that the United States Government retains a non-exclusive, paid-up, irrevocable, world-wide license to publish or reproduce the published form of this manuscript, or allow others to do so, for United States Government purposes. The authors would like to thank Dr Roland Kalb from Proionic for his insightful discussions on the toxicity and recycling of Ionic Liquids.

References

1 E. B. Soriaga, *The crystal and molecular structures of three transition metal complexes*, University of Hawai'i at Manoa, 1978.
2 Plastics - the Facts 2016, PlasticsEurope, https://www.plasticseurope.org/application/files/4315/1310/4805/plastic-the-fact-2016.pdf, (accessed July 30, 2021).
3 World Economic Forum, The New Plastics Economy Rethinking the future of plastics, https://www.weforum.org/press/2016/01/more-plastic-than-fish-in-the-ocean-by-2050-report-offers-blueprint-for-change, (accessed July 30, 2021).

4 P. Villarrubia-Gómez, S. E. Cornell and J. Fabres, *Mar. Policy*, 2018, **96**, 213–220.
5 The COVID-19 pandemic is unleashing a tidal wave of plastic waste 2020, Los Angeles Times, https://www.latimes.com/world-nation/story/2020-06-13/coronavirus-pandemic-plastic-waste-recycling, (accessed July 30, 2021).
6 Breaking the Plastic Wave: Top Findings for Preventing Plastic Pollution, The Pew Charitable Trusts and SYSTEMIQ, https://www.pewtrusts.org/en/research-and-analysis/articles/2020/07/23/breaking-the-plastic-wave-top-findings, (accessed July 30, 2021).
7 M. Patel, N. von Thienen, E. Jochem and E. Worrell, *Resour., Conserv. Recycl.*, 2000, **29**, 65–90.
8 X. Zhang, M. Fevre, G. O. Jones and R. M. Waymouth, *Chem. Rev.*, 2018, **118**, 839–885.
9 J. M. Garcia and M. L. Robertson, *Science*, 2017, **358**, 870–872.
10 A.-C. Albertsson and M. Hakkarainen, *Science*, 2017, **358**, 872–873.
11 S. Weinberger, J. Canadell, F. Quartinello, B. Yeniad, A. Arias, A. Pellis and G. M. Guebitz, *Catalysts*, 2017, **7**, 318.
12 E. Feghali and T. Cantat, *ChemSusChem*, 2015, **8**, 980–984.
13 G. O. Jones, A. Yuen, R. J. Wojtecki, J. L. Hedrick and J. M. Garcia, *Proc. Natl. Acad. Sci. U. S. A.*, 2016, **113**, 7722–7726.
14 X. Qu, G. Zhou, R. Wang, B. Yuan, M. Jiang and J. Tang, *Green Chem.*, 2021, **23**, 1871–1882.
15 N. Sun, R. Parthasarathi, A. M. Socha, J. Shi, S. Zhang, V. Stavila, K. L. Sale, B. A. Simmons and S. Singh, *Green Chem.*, 2014, **16**, 2546–2557.
16 M. Mohan, C. Balaji, V. V. Goud and T. Banerjee, *J. Solution Chem.*, 2015, **44**, 538–557.
17 H. Wang, Z. Li, Y. Liu, X. Zhang and S. Zhang, *Green Chem.*, 2009, **11**, 1568–1575.
18 Q. Yue, C. Wang, L. Zhang, Y. Ni and Y. Jin, *Polym. Degrad. Stab.*, 2011, **96**, 399–403.
19 Q. F. Yue, L. F. Xiao, M. L. Zhang and X. F. Bai, *Polymers*, 2013, **5**, 1258–1271.
20 C. S. Nunes, M. J. V. da Silva, D. C. da Silva, A. d. R. Freitas, F. A. Rosa, A. F. Rubira and E. C. Muniz, *RSC Adv.*, 2014, **4**, 20308–20316.
21 F. Liu, Z. Li, S. Yu, X. Cui and X. Ge, *J. Hazard. Mater.*, 2010, **174**, 872–875.
22 X. Song, F. Liu, L. Li, X. Yang, S. Yu and X. Ge, *J. Hazard. Mater.*, 2013, **244**, 204–208.
23 Q. Wang, X. Yao, S. Tang, X. Lu, X. Zhang and S. Zhang, *Green Chem.*, 2012, **14**, 2559–2566.
24 Q. Wang, X. Yao, Y. Geng, Q. Zhou, X. Lu and S. Zhang, *Green Chem.*, 2015, **17**, 2473–2479.
25 Z. Ju, W. Xiao, X. Lu, X. Liu, X. Yao, X. Zhang and S. Zhang, *RSC Adv.*, 2018, **8**, 8209–8219.
26 C. J. Adams, M. J. Earle and K. R. Seddon, *Green Chem.*, 2000, **2**, 21–24.
27 Y. Liu, X. Yao, H. Yao, Q. Zhou, J. Xin, X. Lu and S. Zhang, *Green Chem.*, 2020, **22**, 3122–3131.
28 J. Sun, N. M. Konda, J. Shi, R. Parthasarathi, T. Dutta, F. Xu, C. D. Scown, B. A. Simmons and S. Singh, *Energy Environ. Sci.*, 2016, **9**, 2822–2834.
29 S. Yoshida, K. Hiraga, T. Takehana, I. Taniguchi, H. Yamaji, Y. Maeda, K. Toyohara, K. Miyamoto, Y. Kimura and K. Oda, *Science*, 2016, **351**, 1196–1199.
30 K. Paduszynski and U. Domanska, *J. Phys. Chem. B*, 2012, **116**, 5002–5018.
31 J. Valderrama and P. Robles, *Ind. Eng. Chem. Res.*, 2007, **46**, 1338–1344.
32 D. M. Eike, J. F. Brennecke and E. J. Maginn, *Ind. Eng. Chem. Res.*, 2004, **43**, 1039–1048.
33 J. K. Shah and E. J. Maginn, *J. Phys. Chem. B*, 2005, **109**, 10395–10405.
34 W. Shi and E. J. Maginn, *J. Phys. Chem. B*, 2008, **112**, 16710–16720.
35 A. Klamt, *J. Phys. Chem.*, 1995, **99**, 2224–2235.
36 A. Klamt and F. Eckert, *Fluid Phase Equilib.*, 2000, **172**, 43–72.
37 M. K. Hadj-Kali, M. Althuluth, S. Mokraoui, I. Wazeer, E. Ali and D. Richon, *Chem. Eng. Commun.*, 2020, **207**, 1264–1277.
38 H. W. Khan, A. V. B. Reddy, M. M. E. Nasef, M. A. Bustam, M. Goto and M. Moniruzzaman, *J. Mol. Liq.*, 2020, **309**, 113122.
39 Y.-R. Liu, K. Thomsen, Y. Nie, S.-J. Zhang and A. S. Meyer, *Green Chem.*, 2016, **18**, 6246–6254.
40 M. Mohan, P. Viswanath, T. Banerjee and V. V. Goud, *Mol. Phys.*, 2018, **116**, 2108–2128.
41 R. S. Kalb, *Commercial Applications of Ionic Liquids*, Springer, 2020, pp. 261–282.
42 M. D. Hanwell, D. E. Curtis, D. C. Lonie, T. Vandermeersch, E. Zurek and G. R. Hutchison, *J. Cheminf.*, 2012, **4**, 17.
43 M. J. Frisch, G. W. Trucks, H. B. Schlegel, G. E. Scuseria, M. A. Robb, J. R. Cheeseman, G. Scalmani, V. Barone, G. A. Petersson, H. Nakatsuji, X. Li, M. Caricato, A. Marenich, J. Bloino, B. G. Janesko, R. Gomperts, B. Mennucci, H. P. Hratchian, J. V. Ortiz, A. F. Izmaylov, J. L. Sonnenberg, D. Williams-Young, F. Ding, F. Lipparini, F. Egidi, J. Goings, B. Peng, A. Petrone, T. Henderson, D. Ranasinghe, V. G. Zakrzewski, J. Gao, N. Rega, G. Zheng, W. Liang, M. Hada, M. Ehara, K. Toyota, R. Fukuda, J. Hasegawa, M. Ishida, T. Nakajima, Y. Honda, O. Kitao, H. Nakai, T. Vreven, K. Throssell, J. A. Montgomery Jr., J. E. Peralta, F. Ogliaro, M. J. Bearpark, J. J. Heyd, E. N. Brothers, K. N. Kudin, V. N. Staroverov, T. A. Keith, R. Kobayashi, J. Normand, K. Raghavachari, A. P. Rendell, J. C. Burant, S. S. Iyengar, J. Tomasi, M. Cossi, J. M. Millam, M. Klene, C. Adamo, R. Cammi, J. W. Ochterski, R. L. Martin, K. Morokuma, O. Farkas, J. B. Foresman and D. J. Fox, *Gaussian 09, Revision D.01*, Gaussian, Inc., Wallingford CT, 2013.
44 M. Mohan, P. K. Naik, T. Banerjee, V. V. Goud and S. Paul, *Fluid Phase Equilib.*, 2017, **448**, 168–177.
45 M. Mohan, T. Banerjee and V. V. Goud, *ACS Omega*, 2018, **3**, 7358–7370.

46 M. Mohan, T. Banerjee and V. V. Goud, *J. Chem. Eng. Data*, 2016, **61**, 2923–2932.
47 M. Gonzalez-Miquel, M. Massel, A. DeSilva, J. Palomar, F. Rodriguez and J. F. Brennecke, *J. Phys. Chem. B*, 2014, **118**, 11512–11522.
48 M. Mohan, V. V. Goud and T. Banerjee, *Fluid Phase Equilib.*, 2015, **395**, 33–43.
49 R. Anantharaj and T. Banerjee, *Ind. Eng. Chem. Res.*, 2010, **49**, 8705–8725.
50 Y. Y. Li and Y. Y. Jin, *Renewable Energy*, 2015, **77**, 550–557.
51 F. Eckert and A. Klamt, *AIChE J.*, 2002, **48**, 369–385.
52 K. A. Kurnia, S. o. P. Pinho and J. o. A. Coutinho, *Ind. Eng. Chem. Res.*, 2014, **53**, 12466–12475.
53 M. Mohan, H. Choudhary, A. George, B. A. Simmons, K. Sale and J. M. Gladden, *Green Chem.*, 2021, **23**, 6020–6035.
54 F. Eckert and A. Klamt, *COSMOtherm, version C3.0 release 19.0.1*, COSMOlogic GmbH & Co KG, Leverkusen, Germany, 2019.
55 C. Loschen and A. Klamt, *Ind. Eng. Chem. Res.*, 2014, **53**, 11478–11487.
56 J. Kahlen, K. Masuch and K. Leonhard, *Green Chem.*, 2010, **12**, 2172–2181.
57 A. Casas, S. Omar, J. Palomar, M. Oliet, M. V. Alonso and F. Rodriguez, *RSC Adv.*, 2013, **3**, 3453–3460.
58 K. X. Huang, M. Mohan, A. George, B. A. Simmons, Y. Xu and J. M. Gladden, *Green Chem.*, 2021, **23**, 6036–6049.
59 H. Wang, G. Gurau and R. D. Rogers, *Chem. Soc. Rev.*, 2012, **41**, 1519–1537.
60 D. G. Raut, O. Sundman, W. Su, P. Virtanen, Y. Sugano, K. Kordas and J.-P. Mikkola, *Carbohydr. Polym.*, 2015, **130**, 18–25.
61 M. Zavrel, D. Bross, M. Funke, J. Büchs and A. C. Spiess, *Bioresour. Technol.*, 2009, **100**, 2580–2587.
62 C. Balaji, T. Banerjee and V. V. Goud, *J. Solution Chem.*, 2012, **41**, 1610–1630.
63 O. Kuzmina, J. Bhardwaj, S. R. Vincent, N. D. Wanasekara, L. M. Kalossaka, J. Griffith, A. Potthast, S. Rahatekar, S. J. Eichhorn and T. Welton, *Green Chem.*, 2017, **19**, 5949–5957.
64 M. Liu, J. Guo, Y. Gu, J. Gao, F. Liu and S. Yu, *ACS Sustainable Chem. Eng.*, 2018, **6**, 13114–13121.
65 H. Ohno and K. Fukumoto, *Acc. Chem. Res.*, 2007, **40**, 1122–1129.
66 J. M. Prausnitz, R. N. Lichtenthaler and E. G. De Azevedo, *Molecular thermodynamics of fluid-phase equilibria*, Pearson Education, 1998.
67 H. Yao, X. Lu, L. Ji, X. Tan and S. Zhang, *Ind. Eng. Chem. Res.*, 2021, **60**, 4180–4188.
68 M. Mohan, T. Banerjee and V. V. Goud, *ChemistrySelect*, 2016, **1**, 4823–4832.
69 J.-M. Andanson, E. Bordes, J. Devémy, F. Leroux, A. A. Pádua and M. F. C. Gomes, *Green Chem.*, 2014, **16**, 2528–2538.
70 F. Furche, R. Ahlrichs, C. Hättig, W. Klopper, M. Sierka and F. Weigend, *Wiley Interdiscip. Rev.: Comput. Mol. Sci.*, 2014, **4**, 91–100.
71 *TURBOMOLE V21.0.1*, University of Karlsruhe and Forschungszentrum Karlsruhe GmbH: Karlsruhe, Germany, 2021, http://www.turbomole.com/.
72 Y. Li, J. Wang, X. Liu and S. Zhang, *Chem. Sci.*, 2018, **9**, 4027–4043.
73 P. Mäki-Arvela, I. Anugwom, P. Virtanen, R. Sjöholm and J.-P. Mikkola, *Ind. Crops Prod.*, 2010, **32**, 175–201.
74 C. Jehanno, I. Flores, A. P. Dove, A. J. Müller, F. Ruipérez and H. Sardon, *Green Chem.*, 2018, **20**, 1205–1212.
75 Understanding REACH, https://echa.europa.eu/regulations/reach/understanding-reach, (accessed 11-16-2021).
76 TSCA Chemical Substance Inventory, https://www.epa.gov/tsca-inventory, (accessed 11-16-2021).
77 D. Coleman and N. Gathergood, *Chem. Soc. Rev.*, 2010, **39**, 600–637.
78 H. Kebaili, A. P. d. l. Ríos, M. J. Salar-Garcia, V. M. Ortiz-Martínez, M. Kameche, J. Hernandez-Fernandez and F. J. Hernández-Fernández, *Front. Mater.*, 2020, 387.
79 C.-W. Cho, T. P. T. Pham, Y.-C. Jeon and Y.-S. Yun, *Green Chem.*, 2008, **10**, 67–72.
80 J. I. Santos, A. M. M. Gonçalves, J. L. Pereira, B. F. H. T. Figueiredo, F. A. e Silva, J. A. P. Coutinho, S. P. M. Ventura and F. Gonçalves, *Green Chem.*, 2015, **17**, 4657–4668.
81 M. Amde, J.-F. Liu and L. Pang, *Environ. Sci. Technol.*, 2015, **49**, 12611–12627.
82 A. J. Greer, J. Jacquemin and C. Hardacre, *Molecules*, 2020, **25**, 5207.
83 J. Zhou, H. Sui, Z. Jia, Z. Yang, L. He and X. Li, *RSC Adv.*, 2018, **8**, 32832–32864.
84 J. M. Rieland and B. J. Love, *Resour., Conserv. Recycl.*, 2020, **155**, 104678.